

Provided for non-commercial research and educational use only.
Not for reproduction or distribution or commercial use.



This article was originally published in a journal published by Elsevier, and the attached copy is provided by Elsevier for the author's benefit and for the benefit of the author's institution, for non-commercial research and educational use including without limitation use in instruction at your institution, sending it to specific colleagues that you know, and providing a copy to your institution's administrator.

All other uses, reproduction and distribution, including without limitation commercial reprints, selling or licensing copies or access, or posting on open internet sites, your personal or institution's website or repository, are prohibited. For exceptions, permission may be sought for such use through Elsevier's permissions site at:

<http://www.elsevier.com/locate/permissionusematerial>

Structural evolution of La–Cr–O thin films: Part I. Microstructure and phase development

Nina Orlovskaya ^{a,*}, Anthony Coratolo ^b, Mykola Lugovy ^b,
Christopher Johnson ^c, Randall Gemmen ^c

^a Michigan Technological University, Department of Materials Science and Engineering, 1400 Townsend Drive, Houghton, MI 49931, USA

^b Drexel University, Department of Materials Science and Engineering, 3141 Chestnut Street, Philadelphia, PA 19104, USA

^c National Energy Technology Laboratory, Department of Energy, 3610 Collins Ferry Road, Morgantown, WV 26507, USA

Received 29 September 2005; received in revised form 25 April 2006; accepted 16 June 2006

Available online 9 August 2006

Abstract

The structural evolution of La–Cr–O thin films and the formation mechanisms of the LaCrO₃ perovskite phase have been studied. X-ray amorphous La–Cr–O protective coatings were deposited by magnetron sputtering on metallic interconnect materials. During the annealing of the material in air a two-step phase transition from La–Cr–O to a monoclinic LaCrO₄ monazite and further to an orthorhombic LaCrO₃ perovskite phase was observed. The formation of a fine nanoporous structure is a result of the significant increase in density of the final LaCrO₃ perovskite in comparison with monazite LaCrO₄ phase. While the porous structure was not sought after for this application, these distinctive nanostructures may have numerous applications in catalysis, separation membranes or for other SOFC components.

© 2006 Published by Elsevier B.V.

Keywords: Ceramics; Coatings; Phase transitions; Sputtering

1. Introduction

LaCrO₃ perovskite ceramics have been the traditional interconnect material for high temperature solid oxide fuel cells (SOFC) which are typically operated at 1000 °C. However, recent advances in new electrolytes [1–3] and electrode materials [4–7] have lead to significant decreases in SOFC operating temperature, and intermediate temperature (650–750 °C) SOFCs have now become a reality. At these operating temperatures, alternative materials, such as chromium-containing iron- or nickel-based metallic alloys have become potential SOFC interconnect materials. The benefits in changing from ceramic to metallic interconnects for SOFC include reduced cost, added reliability, improve electronic conductivity, increased thermal conductivity, and increased stack stability.

The primary drawbacks to commercially available metallic alloys is that they are prone to corrosion and oxidation, and in

the chromium-containing alloys, chromium oxides and hydroxides evaporating from the oxide scale contaminate the cathode and lead to the deterioration of the SOFC. It is therefore necessary to treat the surface either by the addition of reactive elements [8,9], such as La, Ce, Zr and Y, or by coating the surface with a more corrosion-resistant oxide [10,11]. Both of these methods are intended to protect the metallic interconnect against growth of surface oxide layers and prevent chromium evaporation.

There are a number of specific oxide coatings that may provide the necessary oxidation resistance and decrease the volatility of chromium; among these is the material used for interconnects in high temperature SOFCs, LaCrO₃ [12,13]. LaCrO₃-based materials have a good coefficient of thermal expansion (CTE) matched to the substrate and other cell components, are thermodynamically stable, and therefore should reduce chromium volatility. They also have low ionic (O²⁻) conductivity providing good oxidation resistance. The main difficulty with using LaCrO₃ is that it is very difficult to produce dense coatings; however, understanding the phase formation mechanisms in a typical coating may provide

* Corresponding author.

E-mail address: norlovsk@mtu.edu (N. Orlovskaya).

useful information regarding the production of dense chromite coatings.

There are different methods available for the deposition of oxide coatings including magnetron sputtering, pulsed laser deposition, and combustion chemical vapor deposition. In our work, films were deposited using rf magnetron sputtering from LaCrO_3 perovskite targets on to commercially available stainless 446 substrates. This substrate was chosen because of its relatively good CTE match with the coating. During sputtering the substrates were not heated and therefore the “as-deposited” film was found to be amorphous to X-ray diffraction. In order to transform the La–Cr–O amorphous film to the desired orthorhombic LaCrO_3 perovskite phase, the material was heated in air up to 800 °C.

Here we report our findings regarding the La–Cr–O to LaCrO_4 to LaCrO_3 phase transformation. In Part I of this report the microstructure and phase evolution will be explained while in Part II the elasto-plastic characteristics of the films will be reported. The purpose of studying the phase formation mechanism is to direct future efforts in coating technology development. Information regarding the mechanical properties of the coatings may also aid in the development of improved coating technology, as well as allow some predictive capabilities regarding the potentially useful life span of the coated ferritic interconnect materials.

2. Experimental details

Thin films were deposited by magnetron sputtering on the Cr-containing stainless steel (SS) substrates (stainless 446). The magnetron sputtering was performed at Thin Films, Incorporated. Highly porous (40%) light green-colored LaCrO_3 perovskite was used as a target material. The energy dispersive spectroscopy (EDS) analysis of a LaCrO_3 target showed a slight excess of Cr with 49.11 : 50.89 at.% La/Cr ratio. Stainless steel substrates ($10 \times 10 \times 5 \text{ mm}^3$, SS 446) were polished with a diamond spray to a mirror surface. The substrates were coated in the rf sputtering mode under 1 Pa Ar^+ . The substrate temperature was 25 °C at the beginning of deposition. The target to substrate distance was 5 cm. After pre-sputtering the target for 30 min, the substrates were moved into position under the target and then remained stationary. The total time of sputter deposition, at 500 W, was 5 h. Film thickness measured with an Interferometric Surface Profiler, Phase Shift Technology, was $800 \text{ nm} \pm 10\%$. The EDS of an as received film composition gave 56.54 : 43.46 at.% La/Cr ratio. After sputtering, the samples were annealed in air at 500, 600, and 800 °C for 1 h at a controlled heating rate of 30 °C/min (one sample per temperature). The cooling rate after being held at high temperature was 20 °C/min. After annealing at each temperature X-ray diffraction (XRD) data and Raman spectra were acquired from both LaCrO_3 coated and uncoated polished SS samples.

A Siemens diffractometer, with a 1500 W Cu fine focus tube, was used to determine the crystal structure of LaCrO_3 films. Scanning electron microscopy (SEM) and EDS analysis were performed using a FEI/Phillips XL30 scanning electron microscope. The accelerating voltage was 30 kV. The collection

time was 5 min per image. EDS analysis was used to determine the chemical composition of the material investigated. A micro-Raman spectrometer Renishaw 1000 was used to study the vibrational spectra of the film and substrate surfaces. The excitation light was a 514.5 nm line of Ar^+ ion laser with a laser power of 25 mW. The incident and scattered beams were focused using an Olympus microscope with 50 \times objective, which allowed a laser spot size as low as 4–5 μm . All measurements were performed at room temperature. The Raman

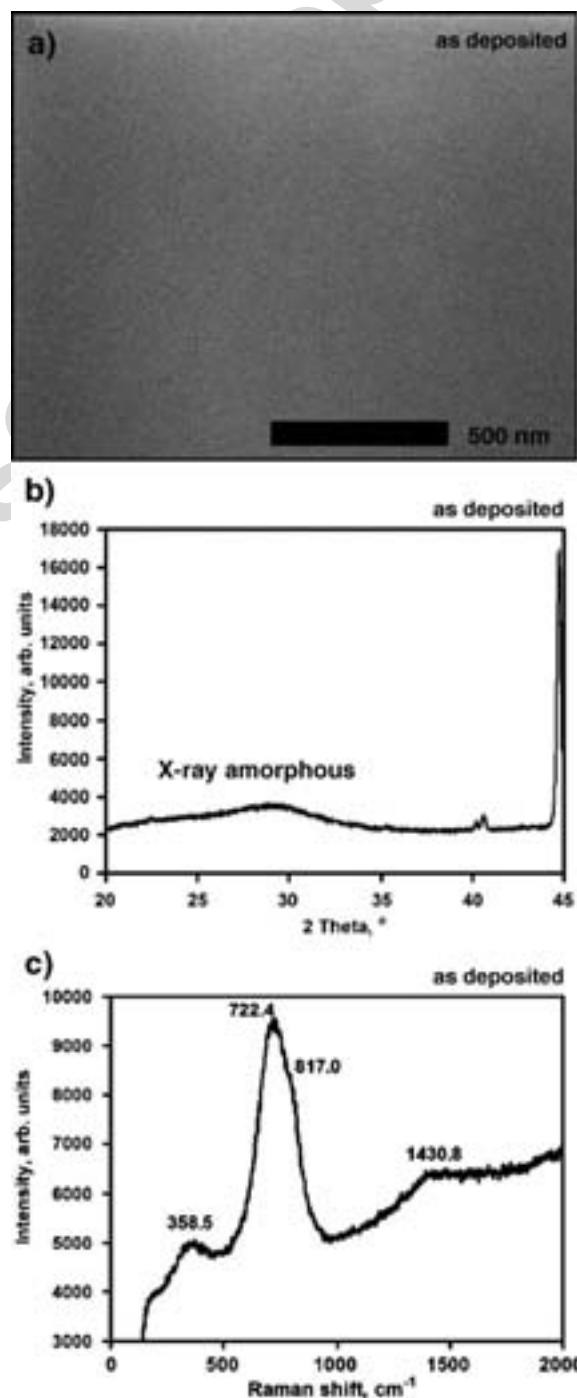


Fig. 1. SEM micrograph (a), X-ray diffraction pattern (b) and Raman spectrum (c) of as deposited La–Cr–O thin film.

bands were deconvoluted using Grams software (Version 4.02 level II 5-31-96).

3. Results and discussion

The “as-deposited” film exhibits a very smooth flat surface with no structural features visible by SEM (Fig. 1a). X-ray diffraction patterns of the as deposited La–Cr–O thin film show no clear crystalline peaks related to the film structure. Peaks at $2\theta=41^\circ$ and 45° belong to the stainless steel substrate material, and a very broad feature with a maximum at $\sim 28^\circ$ may be an indication that while the deposited film is X-ray amorphous, some localized structural features may be present. These local structural features, with a size of 1.5–2 nm, have been observed using transmission electron microscopy dark field imaging [14]. The formation occurs during the deposition of the La–Cr–O thin films by magnetron sputtering, when the substrate temperature was in the range of 200–300 °C. It is known that crystallization of the amorphous film occurs via nucleation and subsequent grain growth [15]. First, local ordering occurs without significant nucleation being required, which then leads to a locally ordered structure composed of medium-range and short-range ordered clusters. The locally ordered structure is more stable than the amorphous phase, but it does not have any characteristics of a crystalline phase, such as clearly visible peaks in the X-ray diffraction pattern or diffraction spots in the transmission electron diffraction pattern. These local structural inhomogeneities in the amorphous state are one of the parameters that control further heterogeneous nucleation and the crystal growth processes during the amorphous–crystalline transition [16]. When local order dominates, the temperature induced transformation leads to a structure composed of very small short- or medium-ranged ordered clusters. The earliest stage of crystallization is the most difficult to observe, yet it can dictate the rest of the growth process [17]. While the “as-deposited” La–Cr–O thin film was X-ray amorphous (Fig. 1b), it appears to be Raman active and several Raman bands have been detected by micro-Raman spectroscopy. Broad bands have been observed at 358.5 cm^{-1} and 1430.8 cm^{-1} , and two stronger overlapping bands have been detected at 722.4 and 817 cm^{-1} (Fig. 1c). These bands indicate that local ordered chemical inhomogeneities exist in the initial amorphous state. The vibrational band at 817 cm^{-1} can be a precursor for the LaCrO_4 phase. The Raman spectrum of LaCrO_4 was analyzed in [18]. It consists of one strong band at $\sim 820\text{ cm}^{-1}$ and several more bands at various wave numbers. It is suggested that the asymmetric broadening of a strong 722.4 band (the shoulder of 817 cm^{-1}) can be used as an indication of the presence of a LaCrO_4 precursor phase.

After the formation of the locally ordered structures during the deposition, further heating initiates long-range ordering (crystallization) of the film, which is dominated by nucleation and grain growth. This process results in the formation of larger precipitates. Both of these processes reduce the free energy of the material, and provide a thermodynamic driving force for crystalline phase formation. After annealing at 500 °C, the first signs of the amorphous to nanocrystalline

structural transition can be detected by micro-Raman and SEM. The visible changes in the film structure are seen in SEM micrographs (Fig. 2a) where some structural features with a size of 50–100 nm appear to be emerging from the smooth amorphous structure of the “as-deposited” film. The film remains X-ray amorphous (Fig. 2b), but there is significant growth of a Raman band at 855 cm^{-1} , during annealing at this temperature (Fig. 2c). The growth of this band is accompanied by an increase in the intensities of bands at 175 and 363 cm^{-1} . While the 855 cm^{-1} band grows, the

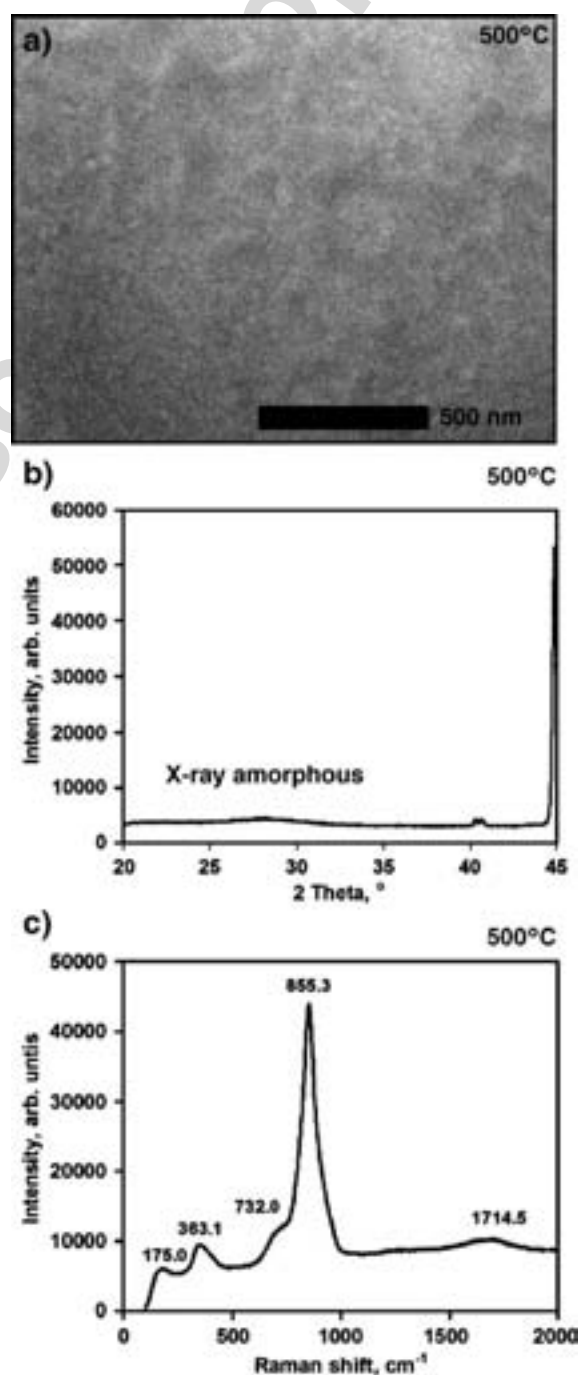


Fig. 2. SEM micrograph (a), X-ray diffraction pattern (b) and Raman spectrum (c) of La–Cr–O thin film annealed at 500 °C.

amorphous phase with bands at 363 and 732 cm^{-1} still remains in the film after annealing at 500 $^{\circ}\text{C}$. This new state can be connected with the beginning of oxygen absorption from air and the formation of the nanocrystalline LaCrO_4 monazite phase. Rare earth chromates, LnCrO_4 (Ln =rare earth), contain unusually high valence state Cr^{V} ions of the d^1 configuration [18]. The $\text{Cr}^{\text{V}}\text{O}_4^{3-}$ tetrahedra in LaCrO_4 have C_1 symmetry of four different Cr–O bond lengths. All four

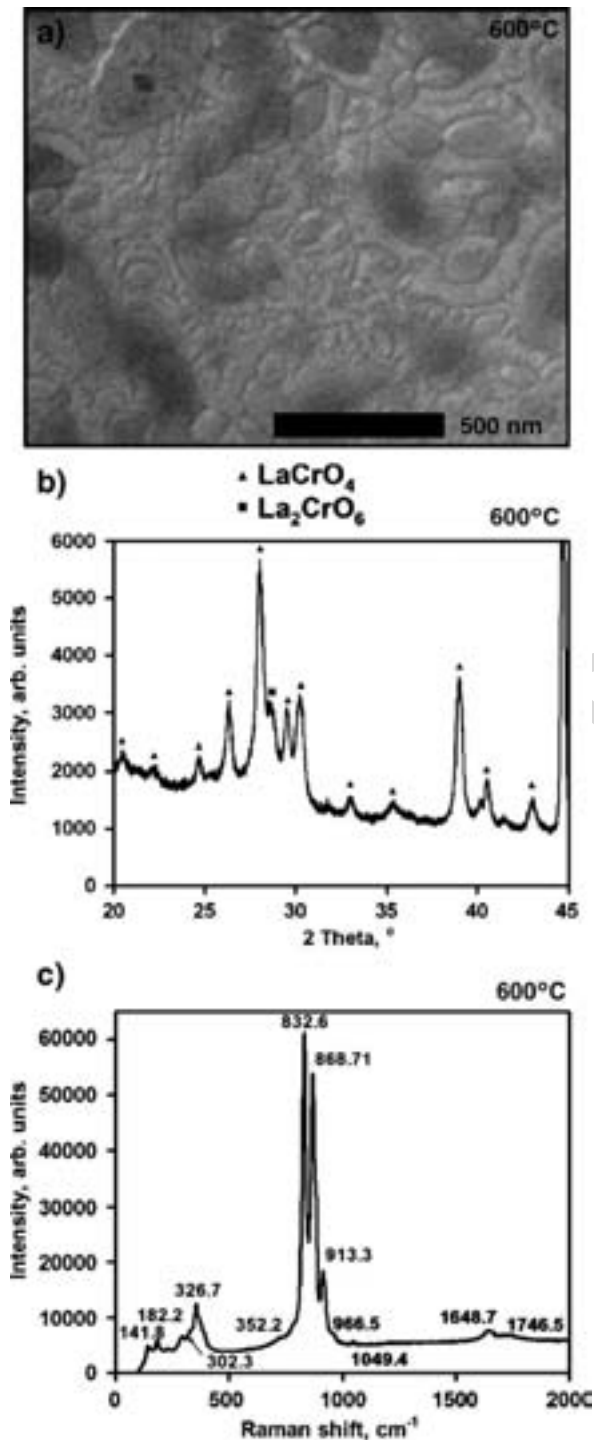


Fig. 3. SEM micrograph (a), X-ray diffraction pattern (b) and Raman spectrum (c) of La–Cr–O thin film annealed at 600 $^{\circ}\text{C}$.

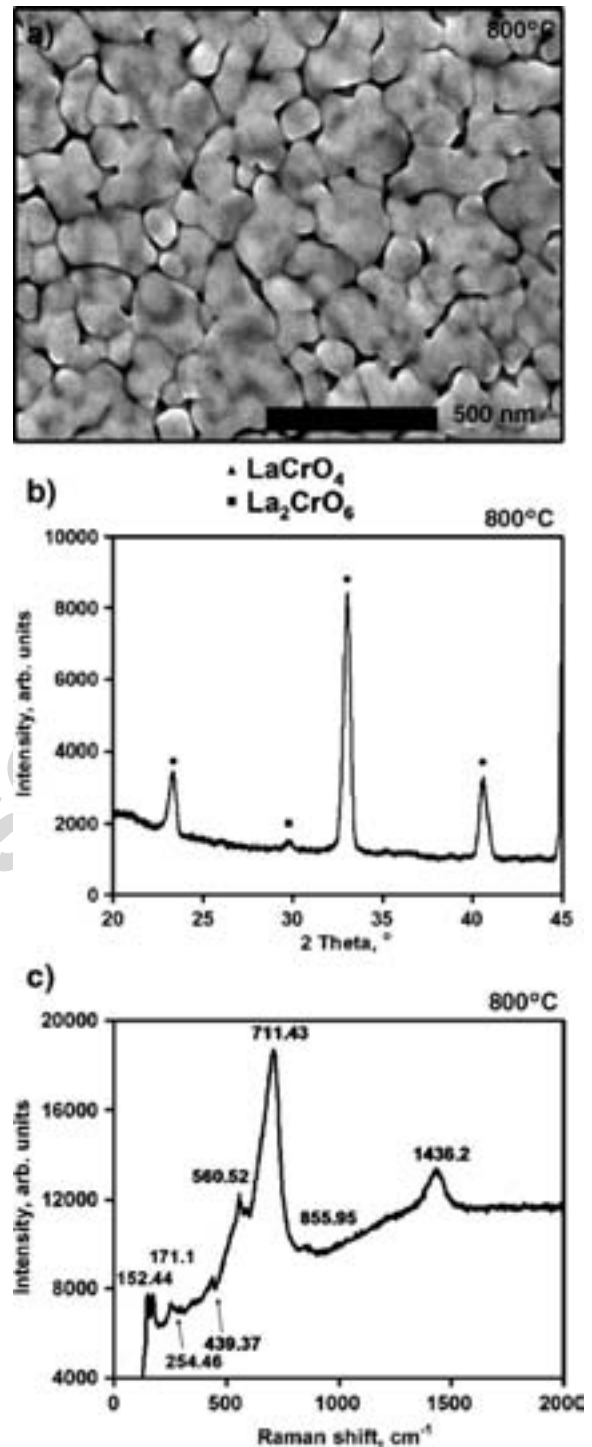


Fig. 4. SEM micrograph (a), X-ray diffraction pattern (b) and Raman spectrum (c) of La–Cr–O thin film annealed at 800 $^{\circ}\text{C}$.

tetrahedral modes are Raman active, and all Raman active modes in LaCrO_4 are related to Cr–O vibration since the bond length of Cr–O is much shorter than that of La–O. While bands at 855 and 363 cm^{-1} are assigned to the LaCrO_4 monazite structure the asymmetric broadening of the 855 cm^{-1} band at the higher wave numbers as well as the appearance of the broad band at 175 cm^{-1} are due to the formation of a small quantity of the La_2CrO_6 structure.

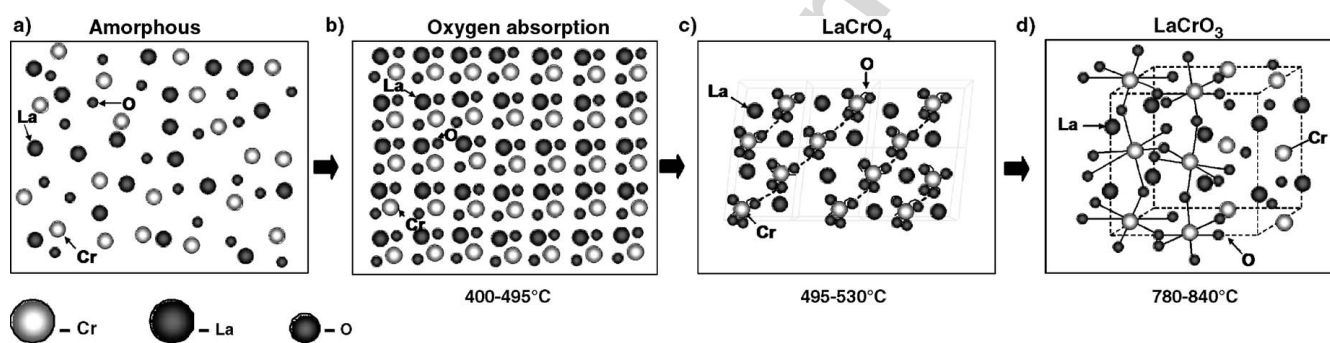


Fig. 5. Schematic presentation of structural development of La-Cr-O thin film upon heating in air.

A fine grain structure is revealed after annealing at 600 °C for 1 h in air (Fig. 3a). The monoclinic LaCrO₄ monazite phase was detected by XRD (Fig. 3b). Some peaks are assigned to the La₂CrO₆ phase. The Raman spectrum of the film is shown in Fig. 3c. The intensities of the Raman bands are very high (up to 100 000 arbitrary units) compared to the intensities of amorphous and nanocrystalline phases (3000 and 10 000 arbitrary units, respectively). Although X-ray analysis reveals that most of the peaks belong to the LaCrO₄ monoclinic phase and the La₂CrO₆ is only a minor constituent, Raman spectroscopy shows that the intensity of the bands (869 cm⁻¹, 913 cm⁻¹) that are assigned to La₂CrO₆ structure [19] are as strong as the intensity of the 832 cm⁻¹ band that belongs to the CrO₄³⁻ tetrahedron stretching mode in LaCrO₄.

When samples were annealed at 800 °C for 1 h in air, a fine self-organized structure, with a significant amount of nanoporosity developed (Fig. 4a). XRD analysis reveals the LaCrO₃ perovskite structure with no preferred orientation, and a small amount of the La₂CrO₆ phase (Fig. 4b). The Raman spectrum of the LaCrO₃ perovskite structure is presented in Fig. 4c. The low energy portion of the Raman vibrational spectrum is assigned to the motion of lanthanum relative to the CrO₆ octahedra [20], and there are two lanthanum internal vibration bands at 152 and 171 cm⁻¹, several weak bands at 254 and 439 cm⁻¹, and two strong bands at 560 and 711 cm⁻¹ that tentatively assigned to the O–Cr–O bending and stretching vibrations. The weak band at 856 cm⁻¹ belongs to La₂CrO₆ residual structure.

It was reported recently that in the case of La–Cr–O compounds, the amorphous to the monoclinic monazite type LaCrO₄ phase transition occurs at 495–530 °C and the reaction is exothermic [21]. Upon further heating the decomposition of LaCrO₄ to the LaCrO₃ perovskite occurs at 780–840 °C. The reaction LaCrO₄ (monoclinic) → LaCrO₃ (orthorhombic) + 0.5O₂ is endothermic and TG data showed a weight decrease that corresponds to the oxygen removal from the lattice [21,22]. The LaCrO₄ decomposition is considered to be composed of the four elementary reactions: a) nucleation and growth of LaCrO₃; b) a phase–boundary reaction between LaCrO₄ and LaCrO₃; c) diffusion of oxygen species through the LaCrO₃ layer; and d) an evolution of O₂ gas. One possible mechanism for the removal of the evolved oxygen is the absorption of the oxygen species onto the LaCrO₃ surface prior to deoxygenation. The molecular volume and theoretical density of LaCrO₄ are 82.30 Å³ molecule⁻¹ and 5.15 g cm⁻³, respectively, and for LaCrO₃ these values are 58.58 Å³ molecule⁻¹ and 6.77 g cm⁻³, respectively [23]. Therefore, the loss of oxygen in LaCrO₄ gives approximately a 30% decrease in molecular volume, which corresponds to about 10% decrease in the grain diameter of LaCrO₃, leading to the observed porosity. It was reported [24], that the LaCrO₄ compound is reversible in a reduction–reoxidation treatment, and, while reduced to Cr³⁺ perovskite structure, could be restored by reoxidation in high oxygen partial pressure atmospheres. In our study, the LaCrO₄ phase dominated as an intermediate product of the amorphous to perovskite structure phase transition. However, another La₂CrO₆ phase was

also detected. The thin film annealed at 800 °C for 1 h showed a LaCrO₃ perovskite structure with a well developed nanoporous structure. Once the LaCrO₃ perovskite phase formed it was stable upon further heat treatment in air and no reversible transition to LaCrO₄ phase has been detected.

The structural changes occurring during the amorphous to crystalline transition may be influenced by the presence of a self-organized network [25]. It was shown that in amorphous materials there are non-random structural networks that go beyond just simple chemical ordering. It was also shown that such networks have the ability to self-organize. Such self-organization decreases the local degrees of freedom of the structure, and removes some constraints in the film [26]. The development of the self-organized model leads to an understanding of the necessity for two phase transitions, and an intermediate phase that should be rigid but stress-free [25]. In the case of the La–Cr–O thin films, it was demonstrated that an amorphous to perovskite structure transition occurs via two steps: the first step is an amorphous to monoclinic LaCrO₄ monazite phase, which is an intermediate phase transition, and a second step when the LaCrO₄ transforms to the LaCrO₃ perovskite. The self-organized structures of the LaCrO₃ perovskite phase are shown to be the results of the processes that occur during the heat-induced crystallization from the amorphous state [12,14].

The schematic representation of the structural development of the La–Cr–O thin film upon heating in air is shown in Fig. 5. Short- to medium-ordered clusters exist after the magnetron deposition of the La–Cr–O thin film, upon annealing at 500 °C the transition to the LaCrO₄ nanophase occurred, followed by the crystallization to the LaCrO₄ phase with some finite amount of the La₂CrO₆ phase by annealing at 600 °C. Annealing at 800 °C, lead to a first order phase transition with a formation of the LaCrO₃ perovskite phase.

4. Conclusion

The nanoporous structure of the perovskite film was obtained by annealing in air an X-ray amorphous La–Cr–O thin film deposited by magnetron sputtering on a stainless steel interconnect material. The deposited film was X-ray amorphous but it underwent a two-step phase transformation to a perovskite structure. The first step is a phase transformation from the X-ray amorphous state to a major intermediate phase: monoclinic LaCrO₄ monazite. A finite amount of La₂CrO₆ phase was also formed. The second step is the transformation of LaCrO₄ into the LaCrO₃ perovskite phase. During this transition nanoporosity appears. These distinctive nanostructures have excellent potential for use in catalysts, SOFCs, and oxygen separation membrane research areas.

Acknowledgement

The financial support of the National Science Foundation through Grant DMR 0502765, NETL, DoE through contract #TSK 41876200101 and NATO through Science for Peace Grant 980878 is acknowledged.

References

- [1] J.-H. Wan, J.-Q. Yan, J.B. Goodenough, *J. Electrochem. Soc.* 152 (2005) A1511.
- [2] K. Huang, J. Goodenough, *J. Alloy. Compd.* 303/304 (2000) 454.
- [3] T. Ishihara, Y. Hiei, Y. Takita, *Solid State Ionics* 79 (1995) 371.
- [4] W.G. Wang, M. Mogensen, *Solid State Ionics* 176 (2005) 457.
- [5] E. Perry Murray, M.J. Sever, S.A. Barnett, *Solid State Ionics* 148 (2002) 27.
- [6] A. Atkinson, S. Barnett, R.J. Gorte, J.T.S. Irvine, A.J. McEvoy, M. Mogensen, C. Singhal, J. Vohs, *Nat. Mater.* 3 (2004) 17.
- [7] S. Tao, J.T.S. Irvine, *Nat. Mater.* 2 (2003) 320.
- [8] P.Y. Hou, J. Stringer, *Mater. Sci. Eng. A202* (1995) 1.
- [9] K. Huang, P.Y. Hou, J.B. Goodenough, *Mater. Res. Bull.* 36 (2001) 81.
- [10] X. Chen, P.Y. Hou, C.P. Jacobson, S.J. Visco, L.C. De Jonghe, *Solid State Ionics* 176 (2005) 425.
- [11] J.H. Zhu, Y. Zhang, A. Basu, Z.G. Lu, M. Paranthaman, D.F. Lee, E.A. Payzant, *Surf. Coat. Technol.* 177–178 (2004) 65.
- [12] N. Orlovskaya, A.M. Coratolo, C. Johnson, R. Gemmen, *J. Am. Ceram. Soc.* 87 (2004) 1981.
- [13] C. Johnson, R. Gemmen, N. Orlovskaya, *Composites. Part B* 35 (2004) 167.
- [14] N. Orlovskaya, A. Nicholls, S. Yarmolenko, J. Sankar, C. Johnson, R. Gemmen, in: N. Sammes, A. Smirnova, O. Vasylyev (Eds.), *Fuel Cells Technologies: State and Perspectives*, Kiev, Ukraine, June 2004, Proceedings of NATO ARW, Kluwer Academic Publishers, 2005, p. 331.
- [15] L. Xing, J. Eckert, W. Loser, *Ann. Chem. Sci. Mater.* 27 (2002) 69.
- [16] H. Touir, J. Dixmier, K. Zellama, J. Morhange, P. Elkaim, *J. Non-Cryst. Solids* 227/230 (1998) 906.
- [17] D.W. Oxtoby, *Nature* 413 (2001) 694.
- [18] Y. Aoki, H. Konno, H. Tachikawa, M. Inagaki, *Bull. Chem. Soc. Jpn.* 73 (2000) 1197.
- [19] Y. Aoki, H. Konno, H. Tachikawa, *J. Mater. Chem.* 11 (2001) 1214.
- [20] D.L. Hoang, A. Dittmar, M. Schneider, A. Trunschke, H. Lieske, K.-W. Brzezinka, K. Witke, *Thermochim. Acta* 400 (2003) 153.
- [21] K. Azegami, M. Yoshinaka, K. Hirota, O. Yamaguchi, *Mater. Res. Bull.* 33 (1998) 341.
- [22] S. Nakayama, M. Sakamoto, *J. Ceram. Soc. Jpn., Int. Ed.* 100 (1992) 342.
- [23] A. Furusaki, H. Konno, R. Furuichi, *Thermochim. Acta* 253 (1995) 253.
- [24] D.L. Hoang, A. Dittmar, J. Radnik, K. Brzezinka, K. Witke, *Appl. Catal., A Gen.* 239 (2003) 95.
- [25] M.F. Thorpe, D.J. Jacobs, M.V. Chubynsky, J.C. Philips, *J. Non-Cryst. Solids* 266/269 (2000) 859.
- [26] Y. Wang, T. Nakaoka, K.S. Murase, *J. Non-Cryst. Solids* 307/310 (2002) 772.